OXFORD

SOT | Society of Toxicology
academic.oup.com/toxsci

TOXICOLOGICAL SCIENCES, 172(1), 2019, 181–190

doi: 10.1093/toxsci/kfz174
Advance Access Publication Date: August 6, 2019
Research Article

Reversibility of Neuroimaging Markers Influenced by Lifetime Occupational Manganese Exposure

David A. Edmondson ,*,† Ruoyun E. Ma,*,†,‡ Chien-Lin Yeh,*,† Eric Ward,* Sandy Snyder,* Elham Azizi,§ S. Elizabeth Zauber,¶ Ellen M. Wells,*,‖ and Ulrike Dydak*,†,1

*School of Health Sciences, Purdue University, West Lafayette, Indiana 47907; †Department of Radiology and Imaging Sciences, Indiana University School of Medicine, Indianapolis, Indiana 46202; ‡Center for Magnetic Resonance Research, University of Minnesota, Minneapolis, Minnesota 55455; §Department of Neurology, Ochsner Medical Center, Kenner, Louisiana 70065; ¶Department of Neurology, Indiana University School of Medicine, Indianapolis, Indiana 46202; and ‖Public Health Graduate Program, Purdue University, West Lafayette, Indiana 47907

The authors certify that all research involving human subjects was done under full compliance with all government policies and the Helsinki Declaration.

[1]To whom correspondence should be addressed. Fax: 765-497-1377; E-mail: udydak@purdue.edu.

ABSTRACT

Manganese (Mn) is a neurotoxicant that many workers are exposed to daily. There is limited knowledge about how changes in exposure levels impact measures in magnetic resonance imaging (MRI). We hypothesized that changes in Mn exposure would be reflected by changes in the MRI relaxation rate R1 and thalamic γ-aminobutyric acid ($GABA_{Thal}$). As part of a prospective cohort study, 17 welders were recruited and imaged on 2 separate occasions approximately 2 years apart. MRI relaxometry was used to assess changes of Mn accumulation in the brain. Additionally, GABA was measured using magnetic resonance spectroscopy in the thalamic and striatal regions of the brain. Air Mn exposure ($[Mn]_{Air}$) and cumulative exposure indexes of Mn (Mn-CEI) for the past 3 months ($Mn\text{-}CEI_{3M}$), past year ($Mn\text{-}CEI_{12M}$), and lifetime ($Mn\text{-}CEI_{Life}$) were calculated using personal air sampling and a comprehensive work history, whereas toenails were collected for analysis of internal Mn body burden. Finally, welders' motor function was examined using the Unified Parkinson's Disease Rating Scale (UPDRS). Median exposure decreased for all exposure measures between the first and second scan. $\Delta GABA_{Thal}$ was significantly correlated with $\Delta Mn\text{-}CEI_{3M}$ ($\rho = 0.66$, adjusted $p = .02$), $\Delta Mn\text{-}CEI_{12M}$ ($\rho = 0.70$, adjusted $p = .006$), and $\Delta[Mn]_{Air}$ ($\rho = 0.77$, adjusted $p = .002$). $\Delta GABA_{Thal}$ significantly decreased *linearly* with $\Delta Mn\text{-}CEI_{3M}$ (quantile regression, $\beta = 15.22$, $p = .02$) as well as $\Delta[Mn]_{Air}$ ($\beta = 1.27$, $p = .04$). Finally, $Mn\text{-}CEI_{Life}$ interacted with $\Delta[Mn]_{Air}$ in the substantia nigra where higher $Mn\text{-}CEI_{Life}$ lessened the ΔR1 per $\Delta[Mn]_{Air}$ (*F*-test, $p = .005$). Although R1 and GABA changed with Mn exposure, UPDRS was unaffected. In conclusion, our study shows that effects from changes in Mn exposure are reflected in thalamic GABA levels and brain Mn levels, as measured by R1, in most brain regions.

Key words: manganese, GABA, magnetic resonance imaging, welding, occupational exposure to manganese, R1.

Excess Mn exposure can lead to a parkinsonian disorder called Manganism, a disease characterized by behavioral, movement, and cognitive impairments, that was first described in cases of chemical plant workers (Couper, 1837). Since Manganism was first described in 1837, exposure levels for workers have been markedly reduced in many countries. Yet, reports of cognitive deficits (Bowler *et al.*, 2006, 2001, 2011; Roels *et al.*, 2012) as well as increases of motor symptoms (Racette *et al.*, 2012b, 2017) due

to Mn exposure are still *status quo*. One population that continues to be exposed to Mn are welders, who are exposed to Mn-containing fumes (Bowler *et al.*, 2006; Cook *et al.*, 1974; Long *et al.*, 2014a; Mena *et al.*, 1967; Racette *et al.*, 2012a). It has been observed that once motor symptoms appear, they remain even after exposure ends and typically do not improve with levodopa treatment (Perl and Olanow, 2007). No alternate form of treatment has been established to date. Therefore, it is necessary to determine whether welders are at risk of Mn toxicity before any symptoms develop.

Having a method that can quantify brain Mn would be ideal as a metric for assessing how Mn contributes to a welder's risk (Meyer-Baron *et al.*, 2013). One possible method uses magnetic resonance imaging (MRI). Due to the paramagnetic properties of Mn, the metal acts as a contrast agent, much like gadolinium, a commonly used contrast agent for diagnostic medical MRI scans (Fornasiero *et al.*, 1987; Silva *et al.*, 2004). Areas with a higher concentration of Mn will show up brighter on a T1-weighted image. Previous studies have shown that brain MRIs of Mn-exposed subjects show increased T1-weighted intensities in the basal ganglia, reflecting Mn accumulation (Bock *et al.*, 2008; Chuang *et al.*, 2009; Criswell *et al.*, 2012; Dorman *et al.*, 2006; Dydak *et al.*, 2011; Lehallier *et al.*, 2012; Long *et al.*, 2014a; Matsuda *et al.*, 2010). However, although the increased intensity is believed to be proportional to Mn accumulation (Dorman *et al.*, 2006), the ability to fully elucidate the relationship has been difficult. Recently, the change in the relaxation rate R1 (where, R1 = 1/T1) was found not to be linearly proportional to lower occupational levels of Mn exposure (Lee *et al.*, 2015), rather reflective of short-term exposure (Lewis *et al.*, 2016).

Another method, magnetic resonance spectroscopy (MRS), measures biochemical concentrations of metabolites and neurotransmitters *in vivo*. γ-aminobutyric acid (GABA), the primary inhibitory neurotransmitter of the central nervous system, has been measured using MRS and was found to be higher in the thalamus of Mn-exposed welders when compared to non-exposed controls (Edmondson *et al.*, 2015; Long *et al.*, 2014b; Ma *et al.*, 2018). A similar result was also found in idiopathic Parkinson's disease (PD) patients (Dydak *et al.*, 2015; O'Gorman Tuura *et al.*, 2018). It is possible that Mn has an effect on nigrostriatal dopaminergic neurons that may trigger an imbalance of neurotransmitters in the basal ganglia, such as changes in GABA concentration in the thalamus (Dharmadhikari *et al.*, 2015; Dydak *et al.*, 2015; Guilarte *et al.*, 2008; Long *et al.*, 2014b; Racette *et al.*, 2011, 2012b), but the effect could also be further downstream in other basal ganglia nuclei. Nonetheless, with work history indicating exposure to Mn, an increase in GABA could potentially be a reliable marker for Mn toxicity. Yet, the GABA levels appear to be dynamic, just as is the exposure, and a single GABA level at 1 time point does not provide enough information about the effect of Mn exposure on the neurotransmitter levels.

Our initial study (Ma *et al.*, 2018) found significantly higher thalamic GABA in highly exposed welders (air exposure > 0.24 mg Mn/m^3) compared to lower exposed welders (mean air exposure 0.13 mg Mn/m^3) and controls. Additionally, R1 was higher in the globus pallidus (GP), substantia nigra (SN), frontal white matter (FWM), and caudate nucleus (CN) in highly exposed welders compared to lower exposed welders and controls. Although thalamic GABA ($GABA_{Thal}$) was correlated with past 3 months and past year Mn exposure windows, R1 was not, thus suggesting that the relationship between R1 and Mn exposure may be complicated by a nonlinear relationship between Mn exposure and Mn accumulation in the brain. To get a better understanding of the dynamic effects of low-level chronic Mn exposure in the workplace, we therefore conducted a longitudinal follow-up study to test the following hypotheses: (1) the change in $GABA_{Thal}$ would be proportional to the change in Mn exposure and (2) the change in R1 would be proportional to the change in Mn exposure.

MATERIALS AND METHODS

This study is a follow-up study of a previous study as described in Ma *et al.* (2018). This study was approved by the Biomedical Institutional Review Board at Purdue University. Written informed consent forms were obtained from all subjects prior to the participation in the study.

Recruitment. Subjects were recruited from the same U.S. truck trailer manufacturer cohort as in Ma *et al.* (2018). Of 32 welders in the first study, 17 male welders ($N = 17$) elected to participate in a follow-up study. All subjects visited the MRI facility for approximately 4 h on a weekend. During this time, they were interviewed about their medical history, work history, and health-related habits (eg, diet, smoking, and drinking). Additionally, they were given a neurological exam from a qualified neurologist and received an MRI scan lasting approximately 1 h in length.

Exposure assessment. Exposure assessment was performed in the welders' workplace with the identical procedure as described in Ma *et al.* (2018) and Ward *et al.* (2018). Briefly, an exposure model using each participant's individual work history combined with air sampling data was used to estimate each participant's Mn cumulative exposure index (Mn-CEI). Average air Mn concentrations for each factory department were estimated using an average of all personal air samples collected from each department. Each personal air sample was collected over the duration of a full work shift (8 h). Our sampling methods used SKC aluminum cyclones with a cut-point of 4 μm, which collects the respirable particles capable of penetrating to the alveolar regions of the lungs, as well as deposit in the brain via the olfactory pathway. The samples were collected inside the welding helmet for welders and on the shoulder in the personal breathing zone for control subjects.

For each participant, the Mn-CEI was calculated as a summation of the individual exposure from the current employer, past employers, and off-the-job welding for the given exposure window in (mg/m^3) years (Ward *et al.*, 2018). Mn-CEIs were calculated for the following exposure time windows: exposure over the past 3 months (before the MRI measurement), exposure over the past year, and cumulative exposure over their working lifetime (back to age 18). The Mn-CEI for the current employer was then calculated by summing over the measured average respirable Mn exposure for each department an individual has worked in during the respective time window, multiplied by the time worked at this department. For cumulative exposure including past employers or for off-the-job welding, the exposure model utilizes additional information from a detailed work history questionnaire, as well as weighting factors accounting for ventilation, welding frequency, welding type, base metals, and use of respirator to better estimate the individual's past exposure based on personal history (Laohaudomchok *et al.*, 2011) For our study, the different exposure windows can be conceptualized (in order of closest to the scan) as recent ($[Mn]_{Air}$, $Mn\text{-}CEI_{3M}$) and distant ($Mn\text{-}CEI_{12M}$, cumulative lifetime Mn exposure $Mn\text{-}CEI_{Life}$).

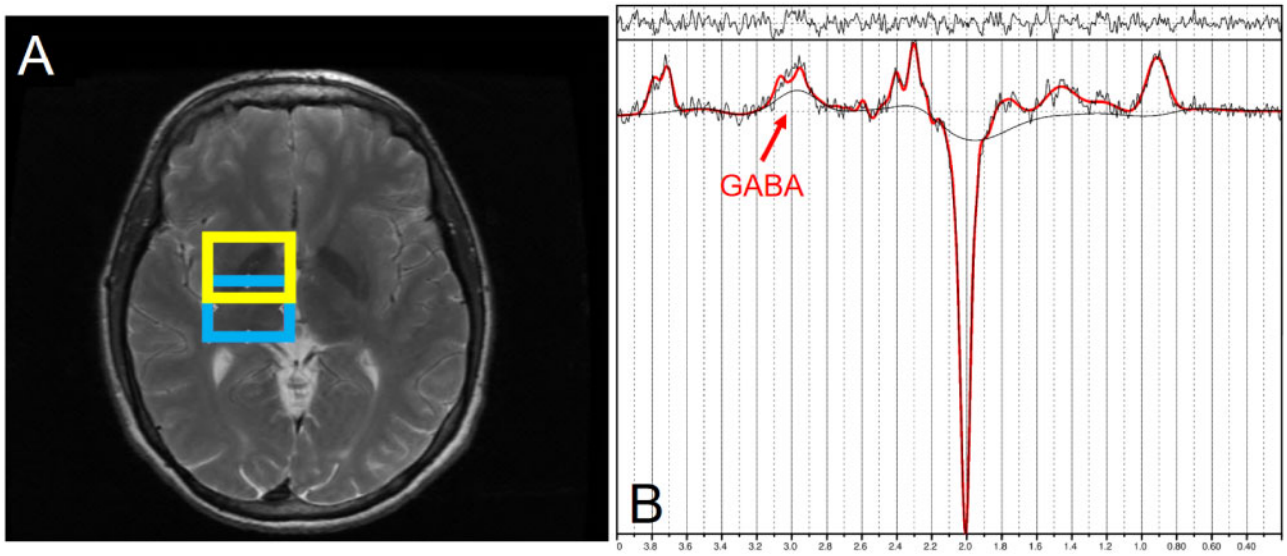

Figure 1. Magnetic resonance spectroscopy (MRS) voxel placement and spectrum. A, Shows the thalamic voxel of interest (VOI) in blue (lower square) and the striatal voxel in yellow (upper square). B, Representative difference spectrum for quantifying γ-aminobutyric acid (GABA) in the thalamic VOI. GABA is indicated by the doublet at 3.0 ppm.

Toenails. Toenail clippings were acquired at the first scan (S1) and second scan (S2) and placed in small envelopes for storage. Analysis of clippings was performed as described in Ward *et al.* (2018), but briefly described here. External contamination was removed using a surfactant solution (1% Triton X-100) for 20 min. After being rinsed with distilled deionized water, the toenails were dried, weighed, and then dissolved by microwave nitric-acid digestion. The digested samples were then analyzed using inductively-coupled plasma mass spectroscopy (ICP-MS). Toenail Mn concentrations ($[Mn]_{Toenail}$) are reported in units of μg/g.

MR spectroscopy. All MRI acquisitions were obtained using a 3T GE Signa MRI scanner with an 8-channel head coil. We obtained GABA-edited spectra using MEGA-PRESS (TR/TE = 2000/68 ms, 256 Averages) (Mullins *et al.*, 2014) in 2 volumes of interest (VOI), thalamic (25 mm × 30 mm × 25 mm) and striatal (25 mm × 30 mm × 25 mm) regions of the brain. Spectra were quantified using LCModel V6.3-1B (Provencher, 1993) and a basis set generated by density matrix simulation using GABA coupling constants from Kaiser *et al.* (2007). The GABA signal in these spectra also includes contributions from coedited macromolecules and homocarnosine and is therefore commonly referred to as GABA+. However, for the sake of simplicity, we refer to the measure as GABA. The thalamus VOI was centered on the right thalamus whereas the striatal VOI was centered over the right striatum, but included parts of the GP, putamen, CN, and thalamus (Figure 1). This overlap was intentional in order to detect any possible contribution of striatal GABA signal in the large thalamus VOI. Water reference scans without water suppression were used for phase and frequency correction. Cerebrospinal fluid (CSF) correction was performed by first segmenting 3D T1-weighted images into 3 components: gray matter (GM), white matter (WM), and CSF (SPM8, Wellcome Department of Imaging Neuroscience, London, United Kingdom). Percentages of each component were calculated for the VOIs using a home-made Matlab code and then GABA levels were corrected for CSF to obtain corrected GABA concentrations (Chowdhury *et al.*, 2014).

Relaxometry. We used MRI relaxometry to assess relative brain Mn accumulation *in vivo*. Whole brain 3D T1 relaxation time mapping was performed using a dual flip angle (3° and 17°) technique (Christensen *et al.*, 1974) consisting of 2 spoiled gradient echo images (SPGR, TR/TE = 6.36/1.76 ms, bandwidth = 2.24 Hz/pixel, matrix dimension = 256 × 192, resolution = 1 mm × 1 mm × 2 mm). Whole brain T1 maps were then generated using an in-house program written in Matlab (The MathWorks, Natick, Massachusetts). T1 was calculated for each pixel based on repetition time (TR), flip angle (a), and a factor that is proportional to the equilibrium longitudinal magnetization (r) (Sabati and Maudsley, 2013). T1 values were calculated in 4 brain regions of interest (ROIs) chosen based on prior studies (Criswell *et al.*, 2012) that showed high Mn deposition in the GP, SN, CN, and FWM. Circular ROIs with an area of 30 mm^2 were measured bilaterally on T1 maps, using the ROI tool in Matlab and Osirix (Pixmeo, Switzerland). R1 values were then calculated as the inverse T1 relaxation time (R1 = 1/T1) and then averaged over left and right hemispheres.

Unified Parkinson's Disease Rating Scale. Subjects' motor abilities were examined by a certified neurologist using the MDS-Unified Parkinson's Disease Rating Scale Part III (UPDRS-III) (Goetz *et al.*, 2007). Rigidity scores were calculated as the summation of 5 items: rigidity in the neck, in the left and right upper extremities, and in the left and right lower extremities. Tremor scores were calculated as the summation of 7 items: left and right kinetic tremor of the hands, rest tremor amplitude in lip/jaw, and rigidity in the right, left, upper, and lower extremities. Bradykinesia scores were calculated as the summation of 5 terms: right and left finger-tapping, right and left hand movements, right and left pronation-supination movements of hands, right and left toe tapping, and right and left leg agility. A higher UPDRS score indicates a worse motor performance with total UPDRS scores 15 or below being considered nonsymptomatic.

Quality assurance. In an effort to ensure all measurements were reliable and stable across both scans, quality assurance (QA) measurements were performed frequently and consistently. These included repeating the MRI and MRS procedures detailed above in phantoms and volunteers. For testing R1, we used a

spherical phantom filled with a solution doped with Mn whereas for testing MRS, we used a spherical phantom filled with a 2.0 mM GABA solution. QA testing showed that R1 measurements in phantoms had a mean of 0.63 s^{-1} with a coefficient of variability (CV) of 15.5%, whereas R1 in volunteers had a mean of 0.64 s^{-1} with a CV of 8%. For GABA, phantoms showed a CV of 2.5% whereas volunteers had a CV of 15%. Voxel placement used specific landmarks within the brain and thus was stable across both time points. CVs across subjects in the thalamic and striatal VOI GM were approximately 15% for both time points, whereas thalamic WM was 7% and striatal WM was 13%. When comparing voxel placement between both scans, there was on average a difference in 0.1% for thalamic and striatal GM and less than 0.1% difference between WM and CSF in each VOI.

Statistical analysis. All statistical tests were performed within the R environment (R Core Team, 2017). A Shapiro-Wilk test of normality was performed on all variables prior to analysis. Mn exposure metrics as well as R1 were nonnormally distributed. Therefore, nonparametric methods were employed when assessing relationships with Mn exposure metrics and R1. Wilcoxon Signed Rank nonparametric tests were used to measure differences in Mn exposure and R1 parameters between S1 and S2. Welch 2 sample *t* tests were uses to assess differences between S1 and S2 in GABA. Differences scores (Δ) were calculated where: Δ = S2 − S1. Spearman partial correlation tests were used to assess correlations between different parameters, such as R1, GABA, and exposure.

For our study we chose to control for cumulative exposure as measured at S2, rather than age at S2. Spearman partial correlation results using age rather than cumulative exposure were virtually identical, with the correlations controlling for cumulative exposure being slightly more significant. Therefore, controlling for cumulative exposure is roughly equivalent to controlling for age, but more relevant in the context of this study. Multiple comparison testing was applied using the Benjamini & Hochberg method ("FDR") to partial correlations. Unadjusted and adjusted *p*-values are presented when applicable.

Due to the small number of subjects and high potential for outliers to affect the results, we assessed linear relationships through nonparametric means using quadratic regressions by estimating the median. To assess interactions, a multiple quantile regression model was used with the included interaction term. For the interaction analysis, the best model was determined by using an *F*-test. Multiple quantile regressions were performed using the *quantreg* package in R.

RESULTS

Exposure assessment for the 17 subjects recruited for a second scan from the original cross-sectional cohort of welders from a local factory (Ma *et al.*, 2018) are shown in Table 1. Welders had an average age of 40.9 (SD = 9.7) years at S1 and 42.4 (SD = 9.7) years at S2.

Changes in Workplace Were Reflected by Changes in Measured Exposure and Imaging Parameters

For the median welder, Mn exposure over the time window 3 months prior to scan, (Mn-CEI_{3M}) decreased by 50% from 0.0.31 (IQR = 0.014–0.048) mg/m^3*year to 0.017 (IQR = 0.006–0.027) mg/m^3*year ($p = .07$); and Mn exposure over the time window 1 year prior to scan (Mn-CEI_{12M}) changed significantly from 0.134 (IQR = 0.066–0.199) mg/m^3*year to 0.067 (IQR = 0.024–0.109) mg/m^3*year ($p = .03$). For the median welder, air Mn concentration ($[Mn]_{Air}$) decreased from 0.110 (IQR = 0.075–0.145) to 0.087 (IQR = 0.079–0.110). Finally, toenail Mn concentration ($[Mn]_{Toenail}$) dropped significantly from 5.63 (IQR = 4.67–7.57) to 5.490 (IQR = 4.375–6.975) μg/g ($p = .02$) (Figure 2).

Table 1. Subject Exposure Assessment

N	Scan 1 17	Scan 2 17
$[Mn]_{Air}$ (mg/m^3)	0.11 (0.075–0.145)	0.087 (0.079–0.110)
$Mn_{Toenail}$ (μg/g)	5.63 (4.67–7.57)	5.49 (4.38–6.98)
Mn-CEI_{3M} (mg/m^3*year)	0.031 (0.014–0.048)	0.017 (0.006–0.027)
Mn-$CEI_{7–12M}$ (mg/m^3*year)	0.055 (0.031–0.069)	0.033 (0.012–0.054)
Mn-CEI_{12M} (mg/m^3*year)	0.134 (0.066–0.199)	0.067* (0.024–0.109)
Mn-CEI_{Life} (mg/m^3*year)	0.875 (0.40–2.441)	1.05 (0.592–2.44)

Median (interquartile range [IQR]) Mn exposure values for all participants. Air Mn and Toenail Mn were directly measured whereas cumulative exposure indexes (CEIs) were estimated using Air Mn and a work history questionnaire. Although all values decreased between Scan 1 and Scan 2, only Mn-CEI_{12M} was significantly lower in Scan 2 ($p = .03$).
*$p < .05$.

Between S1 and S2, R1 values in regions of interest changed dramatically as well. Median R1 lowered in the CN from 0.746 (IQR = 0.70–0.86) s^{-1} to 0.731 (IQR = 0.67–0.77) s^{-1} ($p = .057$), lowered in the GP from 0.936 (IQR = 0.90–0.969) s^{-1} to 0.88 (IQR = 0.84–0.95) s^{-1} ($p = .03$), lowered in the SN from 0.872 (IQR = 0.80–0.921) s^{-1} to 0.72 (IQR = 0.66–0.76) s^{-1} ($p < .0001$), but increased in the FWM from 1.16 (IQR = 1.09–1.23) s^{-1} to 1.42 (1.25–1.55) s^{-1} ($p = .001$). Results are suggesting there was less Mn in most of these regions in S2 compared to S1, with the exception of FWM. Finally, we found that $GABA_{Thal}$ decreased significantly ($p = .0005$) on average from 2.012 to 1.206 mM whereas no significant decrease in striatal GABA could be measured. Taking into account the normal variance in our acquisitions as tested by our phantoms and controls, the changes in $GABA_{Thal}$ (40%) and R1 in the SN (17.3%) and FWM (15.3%) between S1 and S2 were all outside of normal variance expected.

Correlations With Changes in Exposure

To test whether changes in neurochemistry in the brain may be due to changes in Mn exposure, MRS was used to measure changes in neurochemistry in 2 separate voxels within the basal ganglia. In the thalamus voxel, ΔGABA was strongly correlated ($\rho = 0.77$, $p < .0001$, adj. $p = .0002$) with change in air concentration ($\Delta[Mn]_{Air}$) (Figure 3), with the change in exposure 3 months prior to scan (ΔMn-CEI_{3M}) ($\rho = 0.66$, $p = .001$, adj. $p = .02$), and past year (ΔMn-CEI_{12M}) ($\rho = 0.70$, $p = .0004$, adj. $p = .006$), all suggesting that with greater positive changes in Mn exposure, there are corresponding greater positive changes in GABA. In the striatal voxel, ΔGABA was not significantly correlated with any changes in Mn exposure.

To assess whether the change in exposure had any relationship with the observed differences in R1 between S1 and S2, we performed Spearman partial correlations, controlling for cumulative Mn exposure (Mn-CEI_{Life}) at S2. SN R1 had a significant correlation with ΔMn-CEI_{3M} after controlling for cumulative exposure at the S2 ($\rho = 0.50$, $p = .036$, adj. $p = .23$) however this relationship did not survive multiple comparison adjustment (Table 2).

$\Delta[Mn]_{Toenail}$ was significantly correlated ($\rho = 0.64$, $p = .006$, adj. $p = .05$) with the change in Mn exposure 7–12 months prior to scan ($\Delta Mn_{7–12M}$), but was borderline significant after

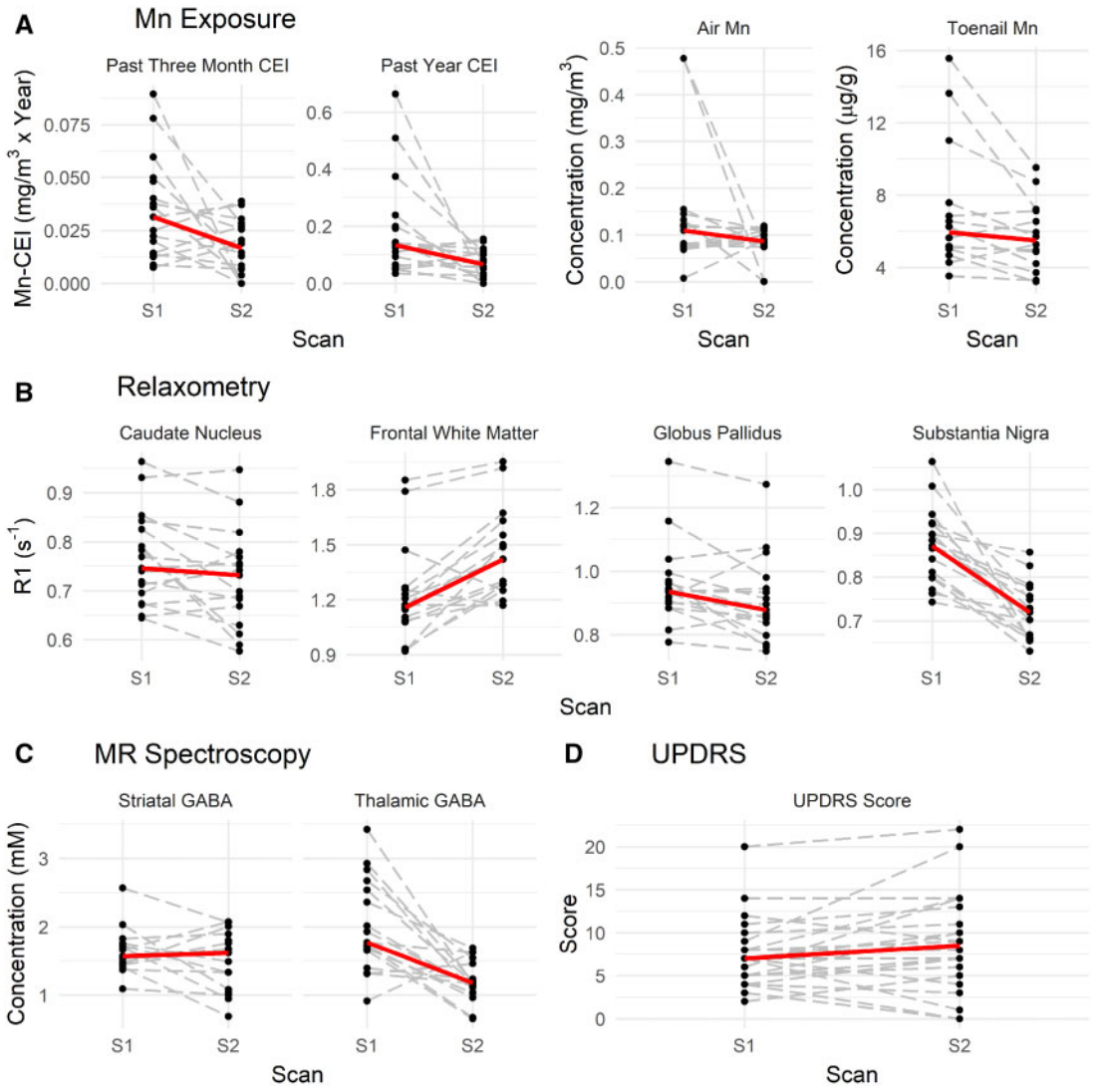

Figure 2. Changes in welders between Scan 1 (S1) and Scan 2 (S2). A, Changes in past 3 months cumulative exposure indexes (CEI) (Mn-CEI_{3M}), past year CEI (Mn-CEI_{12M}), air Mn concentration ($[Mn]_{Air}$), and toenail Mn concentration ($[Mn]_{Toenail}$). B, Changes in R1 in 4 different regions of interest in the brain: caudate nucleus, frontal white matter, globus pallidus, and substantia nigra. C, Changes in γ-aminobutyric acid (GABA) levels in 2 regions of the brain: striatum and thalamus. D, Less changes are observed in Unified Parkinson's Disease Rating Scale (UPDRS) scores. Median trends are the solid line (in red).

adjusting for multiple comparisons. $\Delta[Mn]_{Toenail}$ was not significantly correlated with ΔR1 in any region of interest or ΔGABA in either the thalamic or striatal areas. No significant correlations were found between any Mn exposure metric and UPDRS score.

Linear Relationships Between Mn-CEIs and GABA But Not R1

For relationships that were significantly correlated, an additional test was performed to see if the relationship was linear. Of all significant correlations, only $\Delta GABA_{Thal}$ ($\beta = 15.22$ [95% confidence interval, CI] = 7.45–26.01), p-value = .02) was linearly associated with an increase in ΔMn-CEI_{3M} where for every 0.01 mg/m^3*year change in ΔMn-CEI_{3M} leads to a 0.15 mM median increase in $\Delta GABA_{Thal}$ concentration. $\Delta GABA_{Thal}$ was also linearly associated with an increase in air concentration ($\beta = 1.27$ (95% CI = 0.87–8.22), p-value = .04). For every 0.1 mg/m^3 $\Delta[Mn]_{Air}$, we see a 0.13 mM median increase in $\Delta GABA_{Thal}$ concentration. There were no linear relationships between exposure measurements and ΔR1, including toenails.

Mn-CEI_{Life} Interacts With the Effect of $[Mn]_{Air}$ on R1

After controlling for Mn-CEI_{Life} at S2 in our spearman partial correlations, we wanted to elucidate how a welder's Mn-CEI_{Life} might be affecting the relationship between more recent exposures and R1, GABA, or $[Mn]_{Toenail}$. Therefore, interaction analyses were performed using quantile regression analysis with Mn-CEI_{Life} at S2 included as an interaction term. Using the F-test method to compare regressions with an interaction term and regressions without, we found that for 3 of the 4 tested regions of the brain, Mn-CEI_{Life} had a significant interaction with $\Delta[Mn]_{Air}$ where, as Mn-CEI_{Life} increased, the effect of $\Delta[Mn]_{Air}$ on R1 decreased. In the SN, the median slope of R1 versus $\Delta[Mn]_{Air}$ differed by −0.18 ($p = .005$), by −0.45 in FWM ($p = .04$), and by −0.15 in CN ($p = .009$) for 1 unit change in Mn-CEI_{Life} as measured at S2 (Figure 4). The median slope of R1 versus $\Delta[Mn]_{Air}$ was estimated to differ by $-0.16\,s^{-1}/(mg/m^3)$ ($p = .59$), but this was not significant. Interactions between $\Delta GABA_{Thal}$ and Mn-CEI_{Life} at S2 were also tested. Although not statistically significant, Mn-CEI_{Life} may interact with ΔMn-CEI_{3M}, changing the median slope of

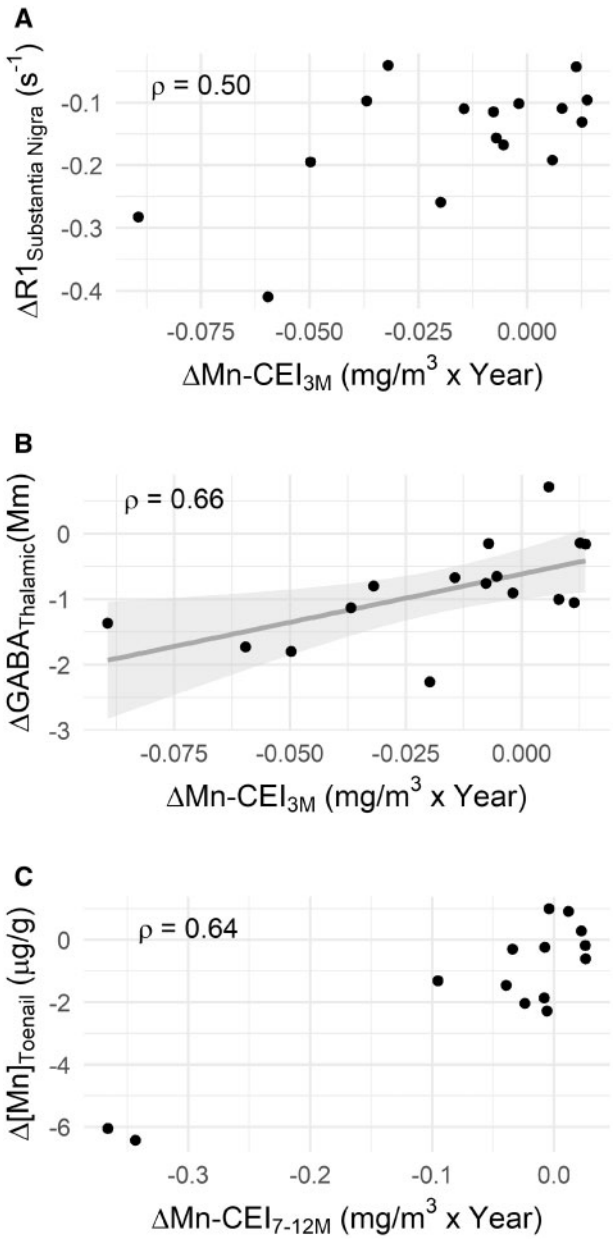

Figure 3. A, Prior to adjusting for multiple comparisons, a significant correlation ($\rho = 0.50$ $p = .036$, adj. $p = .23$) exists between the changes in R1 in the substantia nigra ($\Delta R1_{SN}$) versus the change in Mn exposure at 3 months prior to scan (ΔMn-CEI_{3M}) but no linear relationship. Whereas in (B) there is not only a significant correlation ($\rho = 0.66$, $p = .001$, adj. $p < .02$), but also a linear relationship between the change in thalamic GABA ($\Delta GABA_{Thal}$) and ΔMn-CEI_{3M} ($\beta = 14.7$, $p = .02$). C, Depicts a borderline significant correlation ($\rho = 0.64$, $p = .006$, adj. $p = .05$) between the change in toenail concentration ($\Delta[Mn]_{Toenail}$) and the change in Mn exposure at 7–12 months prior to scan (ΔMn-CEI_{7-12M}).

$\Delta GABA_{Thal}$ versus ΔMn-CEI_{3M} by -4.31 mM/(mg/m^3) ($p = .10$) for 1 unit change in Mn-CEI_{Life}. Finally, there were no interactions between Mn-CEI_{Life} and ΔMn-CEI_{7-12M} for describing $\Delta[Mn]_{Toenail}$ with ΔMn-CEI_{7-12M}. The same interaction tests with age found no significant interaction.

UPDRS Remained Stable Across Both Scans

Although average UPDRS total scores increased between S1 and S2 (7.76–8.88), variability within the scores also increased (standard deviation 4.6–6.06). No correlations or relationships were found between the UPDRS scores (including measured subscores, eg, bradykinesia, tremor, and rigidity) and imaging.

DISCUSSION

Our study measured Mn exposure directly in the workplace, thus we were able to successfully quantify Mn exposure to each participant and measure how exposure levels were changing over time. Significant decreases in Mn exposure were partially due to welders reporting that they were taking more precautionary actions such as by wearing respiratory protection, thus lowering their inhaled Mn exposure. Additionally, many welders went from welding stainless steel to aluminum, thus lowering their Mn exposure virtually to zero. Depending on when this change happened within the 2 years between S1 and S2, it is reflected in Mn-CEI_{3M}, Mn-CEI_{7-12M}, and Mn-CEI_{12M}. Yet, as seen in Table 3 as well as Figure 1, changes of the median over all welders are not large and mostly nonsignificant. This is due to the fact that the direction of these changes is not the same for all subjects. Because this was an observational study in a typical occupational setting (no interference with the work processes or exposure settings of each worker was possible), some welders increased in exposure, whereas others drastically lowered their Mn exposure. Nevertheless, most of the individual welders experienced clear changes in exposure to Mn between the 2 study time points, as well as clear changes in imaging markers, validating the use of correlation analysis between imaging markers and exposures, in spite of nonsignificant changes of the medians.

For example, 3 participants had previously welded in confined tanks with minimal air flow (Table 3). About 6 months after the first round of scanning, 2 of the 3 participants (W1 and W3) went from working in that high Mn environment to welding aluminum, thus dropping their Mn exposure to zero, whereas the third participant (W2) only cut his exposure by approximately one-fifth. The 2 that started welding aluminum had 2 of the largest decreases in $GABA_{Thal}$ as well as in SN R1. The participant that continued to be exposed to Mn had lower SN R1 as well, but change was far less than for the other 2. Relationships between $\Delta GABA_{Thal}$ and $\Delta[Mn]_{Air}$ ($\rho = 0.62$, $p = .008$), as well as $\Delta GABA_{Thal}$ and ΔMn-CEI_{12M} ($\rho = 0.58$, $p = .02$) remained significant even after removing these 3 subjects, however the statistical significance of relationships between $\Delta GABA_{Thal}$ and ΔMn_{3M} ($\rho = 0.44$, $p = .12$) and between $\Delta R1_{SN}$ and ΔMn_{3M} ($\rho = 0.34$, $p = .25$) disappeared. Although these results suggest reversibility, UPDRS increased for the 2 participants that switched to aluminum, whereas the third participant's UPDRS score decreased. Potentially, this could be an effect of age, as the third participant was almost 15 years younger and had less Mn-CEI_{Life} than the other 2.

Prior to adjusting for multiple comparisons, we found that $\Delta R1_{SN}$ correlated with ΔMn_{3M}, which is consistent with another study, which showed that changes in welding hours within 90 days from a scan was associated with changes in R1 after correcting for age, baseline R1, hours worked 90 days before scan, and blood Mn values (Lewis *et al.*, 2016). The same group found that R1 had a nonlinear relationship with hours worked, but that R1 only changed after 300 h welding, or approximately 12 work weeks (Lee *et al.*, 2015), a value similar to our calculated Mn-CEI_{3M}. Due to our sample size and the likelihood of overfitting our data, we were limited in the number of variables we could adjust for within our models. Therefore, after adjusting for multiple comparisons in our study, none of our regions had a directional relationship of R1 with exposure. Although we

Table 2. Spearman Partial Correlation Results

		ΔR1 (s^{-1})				ΔGABA (mM)		
ΔMn Exposure	$\Delta Mn_{Toenail}$ ($\mu g/g$)	GP	SN	FWM	CN	Thalamus	Striatum	UPDRS
$[Mn]_{Air}$ (mg/m^3)	0.18	0.05	0.23	0.22	0.08	**0.77*****	−0.07	0.06
$Mn\text{-}CEI_{3M}$ (mg/m^3*year)	0.10	0.28	0.50	0.32	0.16	**0.66***	−0.10	−0.17
$Mn\text{-}CEI_{7–12M}$ (mg/m^3*year)	**0.64***	0.04	0.12	0.05	−0.15	0.43	0.33	0.20
$Mn\text{-}CEI_{12M}$ (mg/m^3*year)	0.36	0.07	0.23	0.08	−0.13	**0.70****	0.02	0.13

Spearman partial correlations were performed controlling for $Mn\text{-}CEI_{Life}$. Spearman's ρ are shown in this table. Thalamic ΔGABA was significantly correlated with changes in 3 of the 4 exposure windows ($[Mn]_{Air}$,(adj. $p = .0002$) $Mn\text{-}CEI_{3M}$, (adj. $p = .02$) and $Mn\text{-}CEI_{12M}$ (adj. $p = .006$)). Of all regions of interest, only the substantia nigra (SN) finally, $\Delta Mn_{Toenail}$ was significantly correlated with $Mn\text{-}CEI_{7–12M}$ (adj. $p = .05$). Abbreviations: GP, globus pallidus; FWM, frontal white matter; CN, caudate nucleus; UPDRS, Unified Parkinson's Disease Rating Scale.
Adj. p-values: $^{*}p < .05$. $^{**}p < .01$. $^{***}p < .001$.

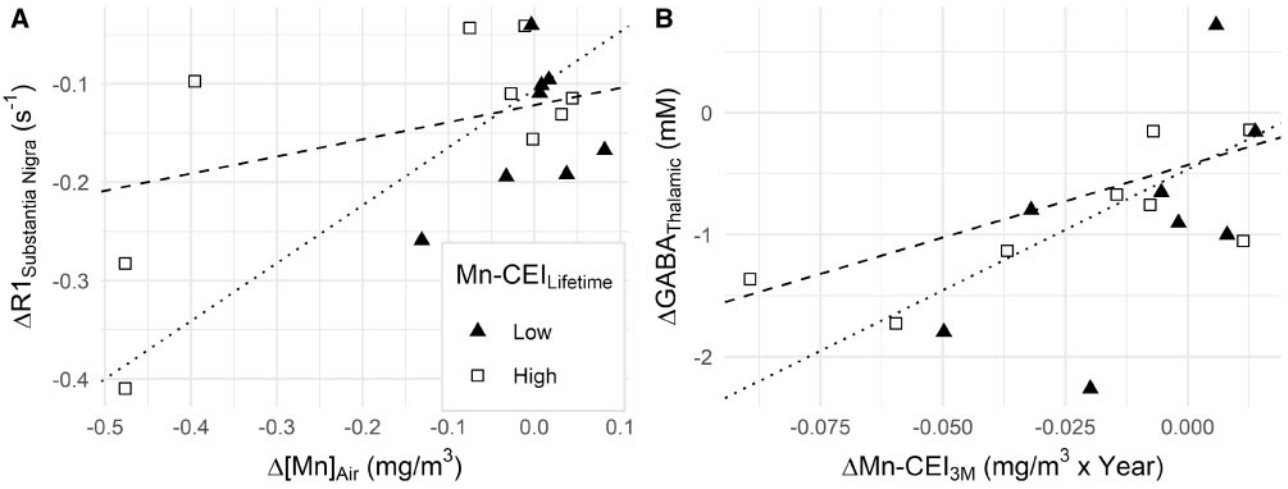

Figure 4. A, The effect of $\Delta[Mn]_{Air}$ on $\Delta R1_{SN}$ is affected significantly by $Mn\text{-}CEI_{Life}$. Subjects with lower levels of $Mn\text{-}CEI_{Life}$ ($\leq 3.15\ mg/m^3 \times year$) have larger $\Delta R1_{SN}$ (triangle, dotted line represents the line of regression for $n = 8$). Subjects with higher levels of $Mn\text{-}CEI_{Life}$ ($> 3.15\ mg/m^3 \times year$) have smaller $\Delta R1_{SN}$ (square, dashed line represents the line of regression for $n = 9$). B, The effect of $\Delta Mn\text{-}CEI_{3M}$ on $\Delta GABA_{Thal}$ is not significantly impacted by $Mn\text{-}CEI_{Life}$.

Table 3. Exposure, UPDRS, and $GABA_{Thal}$ for Welders in Confined Space during First Session

	Manganese																				
	$Mn\text{-}CEI_{3M}$ (mg/m^3*year)			$Mn\text{-}CEI_{7–12M}$ (mg/m^3*year)			$Mn\text{-}CEI_{12M}$ (mg/m^3*year)			$[Mn]_{Air}$ (mg/m^3)			$[Mn]_{Toenail}$ ($\mu g/g$)			UPDRS			$GABA_{Thal}$ (mM)		
	S1	S2	Δ	S1	S2	Δ	S1	S2	Δ	S1	S2	Δ	S1	S2	Δ	S1	S2	Δ	S1	S2	Δ
W1	0.06	0	−0.06	0.095	0	−0.095	0.24	0	−0.24	0.48	0.0003	−0.48	5.02	3.71	−1.31	7	4	−3	2.93	1.20	−1.73
W2	0.05	0.01	−0.04	0.06	0.03	−0.03	0.20	0.05	−0.15	0.48	0.08	−0.40	5.17	4.87	−0.3	10	11	1	2.67	1.54	−1.13
W3	0.09	0	−0.09	0.34	0	−0.34	0.66	0	−0.66	0.48	0.0004	−0.48	13.64	7.21	−6.43	11	13	2	2.54	1.18	−1.36

Three welders performed work in a confined space leading them to having relatively higher Mn exposure measures during the first session (S1). Subjects were then moved out of this work into areas with lower Mn exposure measures.
Abbreviation: UPDRS, Unified Parkinson's Disease Rating Scale.

found that $\Delta GABA_{Thal}$ is linear to $\Delta Mn\text{-}CEI_{3M}$, there is no linear relationship between ΔR1 and any measure of ΔMn-CEI or $\Delta[Mn]_{Air}$.

As shown in biological models, Mn exists in 2 different states in tissue, bound (Mn-B) and free (Mn-F) (Nong *et al.*, 2008, 2009; Ramoju *et al.*, 2017; Schroeter *et al.*, 2012; Taylor *et al.*, 2012; Teeguarden *et al.*, 2007). Mn-B has been bound to proteins or sequestered in vacuoles and thus is less able to diffuse out of a particular region in the brain and affect R1. Mn-F is able to diffuse in and out of the region, and readily interact with the hydrogen spins in water that were excited by MRI, thus increasing the relaxation rate R1. Therefore, R1 changes based on the amount of Mn-F available and the amount of binding sites available for binding Mn-F in each region. At higher exposures, more Mn will accumulate in the brain, with higher preference toward the inner-brain regions such as the basal ganglia and brainstem (Bock *et al.*, 2008), as well as in areas with higher concentrations of Mn-susceptible transporter proteins, such as divalent metal transporter 1 (DMT1) (Au *et al.*, 2008). Eventually, the number of available binding locations will be occupied by Mn-B, forcing

additional Mn to exist in a free state. This Mn-F leads to higher R1 in the region. When Mn-F leaves the region, the R1 decreases proportionately, but Mn-B remains, potentially returning to a free state, thus complicating the relationship between ΔR1 and changes in Mn exposure.

These different states of Mn may explain why we found that at higher levels of Mn-CEI_{Life}, there is less ΔR1 with the $\Delta[Mn]_{Air}$ in all regions except for the GP. Past studies do not implicate previous exposures to Mn as a risk factor to the effects from current exposure. One explanation could be that Mn-CEI_{Life} could potentially change expressions of proteins within the astrocytes and other glial cells, thus affecting the exchange of Mn-B to Mn-F. Changes in protein expression have been shown to occur with higher doses in cell lines, where Mn and Fe dosing caused higher expression of DMT1 (Au *et al.*, 2008). Once transported into the cell, Mn is bound into endosomes for future use. The GP is highly concentrated with another transporter known to accumulate Mn, voltage activated Ca^{2+} channels, and thus there is no interaction of Mn-CEI_{Life} with the effect of more recent windows of exposure on ΔR1 at our exposure levels.

We also found that $\Delta[Mn]_{Toenail}$ changed proportionately with the ΔMn-$CEI_{7–12M}$, further validating the use of toenails as a biomarker for Mn-$CEI_{7–12M}$ prior to clipping. Because there were no statistically significant relationships between $\Delta[Mn]_{Toenail}$ and R1 in any region or between $\Delta[Mn]_{Toenail}$ and GABA, this suggests that the accumulation of toenail Mn over a given time represents a separate time window of exposure compared to either R1 or GABA. Additionally, we found that the relationship between $\Delta[Mn]_{Toenail}$ and ΔMn-$CEI_{7–12M}$ was not affected by Mn-CEI_{Life}, suggesting that the process by which Mn accumulates in toenails is different than how it accumulates in brain regions, or affects R1.

$\Delta R1_{FWM}$ performed the opposite of what was expected, with R1 increasing in FWM for many people between S1 and S2 rather than going down proportionally to the change in exposure. Mn has been used for decades now in Mn-enhanced MRI, or MEMRI, as a contrast agent in preclinical studies particularly for tracing neurons due to anterograde Mn transport along axons. In a recent study using whole brain R1 mapping to compare welders and controls, R1 is significantly higher for welders compared to controls along white matter tracks (Yeh *et al.*, 2016). Because the striatum has many neuronal projections to the frontal cortex, the excess Mn may have migrated to the FWM. Anterograde transport of Mn to the FWM would cause an increase in R1 that cannot be accounted for by the differences in recent Mn exposure due to our 2 time points being approximately 2 years apart.

We also found that GABA changes proportionately with Mn exposure. $\Delta GABA_{Thal}$ correlated with all measurements of $\Delta[Mn]_{Air}$ or ΔMn-CEI after correcting for Mn-CEI_{Life} at S2. Additionally, there was a significant linear relationship between $\Delta GABA_{Thal}$ and changes in $[Mn]_{3M}$. Therefore, $\Delta GABA_{Thal}$ could be considered reflective of changes in the workplace environment's Mn exposure levels. For instance, as participants were exposed to less Mn in the air, by the time of S2, their $GABA_{Thal}$ subsided to levels similar to controls in our previous study (Ma *et al.*, 2018). In that study, it was concluded that higher levels of $GABA_{Thal}$ in welders likely represented a dysregulation of neurotransmitters in the basal ganglia. Although we see reversal of GABA levels coexisting with lower exposure levels, UPDRS scores did not change proportionately, suggesting that while $GABA_{Thal}$ is reversible, neurological dysfunction is not. However, we did not see any observable changes in striatal GABA levels. This may be because the striatal VOI contains many regions of the basal ganglia, including both GP internal and external. According to the pathways within the basal ganglia (Gerfen and Bolam, 2016), we assume that there could be opposing changes of GABA levels in these subareas that we cannot separate within out voxel.

One reason for why $GABA_{Thal}$ changes with Mn exposure may be due to upstream Mn accumulation in the GP or SN causing downstream effects in the thalamus. There has been evidence that Mn inhibited calcium-dependent release of GABA (Cotman *et al.*, 1976) and increased GABA has been reported in earlier articles after exposure to Mn (Bonilla, 1978). Because the GP has a higher concentration of Ca^{2+} channels, this could be the initial point of toxicity. Mn may impair GABAergic neurons projecting from the GP, leading to an increase in GABA in the thalamus.

Although this study had a small sample size of 17, the strength of our longitudinal design allowed for each of our welders to effectively be their own control. Additionally, this study design removed the need to account for potential confounders, such as diet or smoking, making this study much stronger than an observational study design. One limitation, though, is that our CEIs become less precise the further their windows extend into the past. Additionally, we are limited by the resolution of MRS to obtain meaningful GABA concentrations in regions of the basal ganglia, besides the thalamus. In conclusion, our study shows that effects from changes in Mn exposure are reflected in thalamic GABA levels and brain Mn levels, as measured by R1, in most brain regions.

In conclusion, our study shows that dynamic effects from Mn exposure can be measured using a longitudinal study design incorporating MRI and MRS. We show that changes in levels of $GABA_{Thal}$ and region-specific R1 are largely proportional to environmental exposure to Mn. When exposure decreases, GABA decreases as well—showing that the change in GABA is a potential biomarker for the effects of Mn exposure. As the exposure decreases, R1 also decreases in most regions, except for FWM. Although the change is not linearly proportional to the change in Mn exposure, an appropriate model might be able to explain the changes. But, the model will need to take into account Mn-CEI_{Life}, as we have some evidence that this influences the turnover rate of Mn in the brain.

DECLARATION OF CONFLICTING INTERESTS

The authors declared no potential conflicts of interest with respect to the research, authorship, and/or publication of this article.

FUNDING

Funding for this study was provided by National Institute of Environmental Health Sciences (R01 ES020529, F31 ES028081); CDC/ National Institute for Occupational Safety and Health (T03 OH008615).

REFERENCES

Au, C., Benedetto, A., and Aschner, M. (2008). Manganese transport in eukaryotes: The role of DMT1. *NeuroToxicology* **29**, 569–576.

Bock, N. A., Paiva, F. F., Nascimento, G. C., Newman, J. D., and Silva, A. C. (2008). Cerebrospinal fluid to brain transport of manganese in a non-human primate revealed by MRI. *Brain Res.* **1198**, 160–170.

Bonilla, E. (1978). Increased GABA content in caudate nucleus of rats after chronic manganese chloride administration. *J. Neurochem*. **31**, 551–552.

Bowler, R., Gocheva, V., Harris, M., Ngo, L., Abdelouahab, N., Wilkinson, J., Doty, R. L., Park, R., and Roels, H. A. (2011). Prospective study on neurotoxic effects in manganese-exposed bridge construction welders. *NeuroToxicology* **32**, 596–605.

Bowler, R., Gysens, S., Diamond, E., Nakagawa, S., Drezgic, M., and Roels, H. A. (2006). Manganese exposure: Neuropsychological and neurological symptoms and effects in welders. *NeuroToxicology* **27**, 315–326.

Bowler, R., Lezak, M., Booty, A., Hartney, C., Mergler, D., Levin, J., and Zisman, F. (2001). Neuropsychological dysfunction, mood disturbance, and emotional status of munitions workers. *Appl. Neuropsychol*. **8**, 74–90.

Chowdhury, F. A., O'Gorman, R. L., Nashef, L., Elwes, R. D., Edden, R. A., Murdoch, J. B., Barker, G. J., and Richardson, M. P. (2014). Investigation of glutamine and GABA levels in patients with idiopathic generalized epilepsy using MEGAPRESS. *J. Magn. Reson. Imaging* **699**, 694–699.

Christensen, K. A., Grant, D. M., Schulman, E. M., and Walling, C. (1974). Optimal determination of relaxation times of Fourier transform nuclear magnetic resonance. Determination of spin-lattice relaxation times in chemically polarized species. *J. Phys. Chem*. **78**, 1971–1977.

Chuang, K.-H., Koretsky, A. P., and Sotak, C. H. (2009). Temporal changes in the T1 and T2 relaxation rates (ΔR1 and ΔR2) in the rat brain are consistent with the tissue-clearance rates of elemental manganese. *Magn. Reson. Med*. **61**, 1528–1532.

Cook, D., Fahn, S., and Brait, K. (1974). Chronic manganese intoxication. *Arch Neurol*. **30**, 59–64.

Cotman, C. W., Haycock, J. W., and White, W. F. (1976). Stimulus-secretion coupling processes in brain: Analysis of noradrenaline and gamma-aminobutyric acid release. *J. Physiol*. **254**, 475–505.

Couper, J. (1837). On the effects of black oxide of manganese when inhaled into the lungs. *Br. Ann. Med. Pharm. Vital Stat. Gen. Sci*. **1**, 41–42.

Criswell, S. R., Perlmutter, J. S., Huang, J. L., Golchin, N., Flores, H. P., Hobson, A., Aschner, M., Erikson, K. M., Checkoway, H., and Racette, B. A. (2012). Basal ganglia intensity indices and diffusion weighted imaging in manganese-exposed welders. *Occup. Environ. Med*. **69**, 437–443.

Dharmadhikari, S., Ma, R., Yeh, C.-L., Stock, A.-K., Snyder, S., Zauber, S. E., Dydak, U., and Beste, C. (2015). Striatal and thalamic GABA level concentrations play differential roles for the modulation of response selection processes by proprioceptive information. *NeuroImage* **120**, 36–42.

Dorman, D. C., Struve, M. F., Wong, B. A., Dye, J. A., and Robertson, I. D. (2006). Correlation of brain magnetic resonance imaging changes with pallidal manganese concentrations in rhesus monkeys following subchronic manganese inhalation. *Toxicol. Sci*. **92**, 219–227.

Dydak, U., Dharmadhikari, S., Snyder, S., and Zauber, S. E. (2015). Increased thalamic GABA levels correlate with Parkinson Disease severity. In *AD/PD Conference*. Nice, France.

Dydak, U., Jiang, Y., Long, L., Zhu, H., Chen, J., Li, W., Edden, R., Hu, S., Fu, X., Long, Z., *et al.* (2011). In vivo measurement of brain GABA concentrations by magnetic resonance spectroscopy in smelters occupationally exposed to manganese. *Environ. Health Perspect*. **119**, 219–224.

Edmondson, D., Ma, R., Yeh, C.-L., Ward, E. J., Snyder, S., Zauber, S. E., Rosenthal, F., and Dydak, U. (2015). Increased GABA levels in manganese-exposed welders correlate with exposure, brain manganese, cognitive function, and motor function. *Neurotoxicol. Teratol*. **49**, 121.

Fornasiero, D., Bellen, J., Baker, R., and Chatterton, B. (1987). Paramagnetic complexes of manganese (II), iron (III), and gadolinium (III) as contrast agents for magnetic resonance imaging. *Invest. Radiol*. **22**, 322–327.

Gerfen, C., and Bolam, J. (2016). The neuroanatomical organization of the basal ganglia. In *Handbook of Basal Ganglia Structure and Function* (H. Steiner and K. Tseng, Eds.), 2nd ed, pp. 3–31. Elsevier, Amsterdam.

Goetz, C.G., Fahn, S., Matrinez-Martin, P., Poewe, W., Sampaio, C., Stebbins, G.T., Stern, M.B., Tilley, B.C., Dodel, R., Dubois, B., et al. 2007. Movement Disorder Society-sponsored revision of the Unified Parkinson's Disease Rating Scale (MDS-UPDRS): Process, format, and clinimetric testing plan. *Mov. Disord*. **22**, 41–47.

Guilarte, T. R., Burton, N. C., McGlothan, J. L., Verina, T., Zhou, Y., Alexander, M., Pham, L., Griswold, M., Wong, D. F., Syversen, T., *et al.* (2008). Impairment of nigrostriatal dopamine neurotransmission by manganese is mediated by pre-synaptic mechanism(s): Implications to manganese-induced Parkinsonism. *J. Neurochem*. **107**, 1236–1247.

Kaiser, L.G., Young, K., and Matson, G.B. (2007). Elimination of spatial interference in PRESS-localized editing spectroscopy. Magn. Reson. Med. **58**, 813–818.

Laohaudomchok, W., Lin, X., Herrick, R. F., Fang, S. C., Cavallari, J. M., Shrairman, R., Landau, A., Christiani, D. C., and Weisskopf, M. G. (2011). Neuropsychological effects of low-level manganese exposure in welders. *NeuroToxicology* **32**, 171–179.

Lee, E.-Y., Flynn, M. R., Du, G., Lewis, M. M., Fry, R., Herring, A. H., Van Buren, E., Van Buren, S., Smeester, L., Kong, L., *et al.* (2015). T1 relaxation rate (R1) indicates nonlinear Mn accumulation in brain tissue of welders with low-level exposure. *Toxicol. Sci*. **146**, 281–289.

Lehallier, B., Coureaud, G., Maurin, Y., and Bonny, J.-M. (2012). Effects of manganese injected into rat nostrils: Implications for in vivo functional study of olfaction using MEMRI. *Magn. Reson. Imaging* **30**, 62–69.

Lewis, M. M., Flynn, M. R., Lee, E. Y., Van Buren, S., Van Buren, E., Du, G., Fry, R. C., Herring, A. H., Kong, L., Mailman, R. B., *et al.* (2016). Longitudinal T1 relaxation rate (R1) captures changes in short-term Mn exposure in welders. *NeuroToxicology* **57**, 39–44.

Long, Z., Jiang, Y.-M., Li, X.-R., Fadel, W., Xu, J., Yeh, C.-L., Long, L.-L. L., Luo, H.-L., Harezlak, J., Murdoch, J. B., *et al.* (2014a). Vulnerability of welders to manganese exposure—A neuroimaging study. *NeuroToxicology* **45**, 285–292.

Long, Z., Li, X.-R., Xu, J., Edden, R., Qin, W.-P., Long, L.-L. L., Murdoch, J. B., Zheng, W., Jiang, Y.-M., and Dydak, U. (2014b). Thalamic GABA predicts fine motor performance in manganese-exposed smelter workers. *PLoS One* **9**, e88220.

Ma, R. E., Ward, E. J., Yeh, C.-L., Snyder, S., Long, Z., Gokalp Yavuz, F., Zauber, S. E., and Dydak, U. (2018). Thalamic GABA levels and occupational manganese neurotoxicity: Association with exposure levels and brain MRI. *NeuroToxicology* **64**, 30–42.

Matsuda, K., Wang, H. X., Suo, C., McCombe, D., Horne, M. K., Morrison, W. A., and Egan, G. F. (2010). Retrograde axonal tracing using manganese enhanced magnetic resonance imaging. *NeuroImage* **50**, 366–374.

Mena, I., Marin, O., Fuenzalida, S., and Cotzias, G. (1967). Chronic manganese poisoning. clinical picture and manganese turnover. *Neurology* **17**, 128–136.

Meyer-Baron, M., Schäper, M., Knapp, G., Lucchini, R., Zoni, S., Bast-Pettersen, R., Ellingsen, D. G., Thomassen, Y., He, S., Yuan, H., *et al.* (2013). The neurobehavioral impact of manganese: Results and challenges obtained by a meta-analysis of individual participant data. *NeuroToxicology* **36**, 1–9.

Mullins, P. G., Mcgonigle, D. J., O'Gorman, R. L., Puts, N. A., Vidyasagar, R., Evans, C. J., Edden, R., Brookes, M. J., Garcia, A., Foerster, B. R., *et al.* (2014). Current practice in the use of MEGA-PRESS spectroscopy for the detection of GABA. *NeuroImage* **86**, 43–52.

Nong, A., Taylor, M. D., Clewell, H. J., Dorman, D. C., and Andersen, M. E. (2009). Manganese tissue dosimetry in rats and monkeys: Accounting for dietary and inhaled Mn with physiologically based pharmacokinetic modeling. *Toxicol. Sci.* **108**, 22–34.

Nong, A., Teeguarden, J. G., Clewell, H. J., Dorman, D. C., and Andersen, M. E. (2008). Pharmacokinetic modeling of manganese in the rat IV: Assessing factors that contribute to brain accumulation during inhalation exposure. *J. Toxicol. Environ. Health A* **71**, 413–426.

O'Gorman Tuura, R. L., Baumann, C. R., and Baumann-Vogel, H. (2018). Neurotransmitter activity is linked to outcome following subthalamic deep brain stimulation in Parkinson's disease. *Parkinsonism Relat. Disord.* **50**, 54–60.

Perl, D. P., and Olanow, C. W. (2007). The neuropathology of manganese-induced Parkinsonism. *J. Neuropathol. Exp. Neurol.* **66**, 675–682.

Provencher, S. W. (1993). Estimation of metabolite concentrations from localized in vivo proton NMR spectra. *Magn. Reson. Med.* **30**, 672–679.

R Core Team (2017). *R: A language and environment for statistical computing*. R Foundation for Statistical Computing Vienna, Austria. https://www.R-project.org/.

Racette, B. A., Aschner, M., Guilarte, T. R., Dydak, U., Criswell, S. R., and Zheng, W. (2012a). Pathophysiology of manganese-associated neurotoxicity. *NeuroToxicology* **33**, 881–886.

Racette, B. A., Criswell, S. R., Lundin, J. I., Hobson, A., Seixas, N., Kotzbauer, P. T., Evanoff, B. A., Perlmutter, J. S., Zhang, J., Sheppard, L., *et al.* (2012b). Increased risk of Parkinsonism associated with welding exposure. *NeuroToxicology* **33**, 1356–1361.

Racette, B. A., Criswell, S. R., Perlmutter, J. S., Videen, T. O., Moerlein, S. M., Flores, H. P., Birke, A. M., and Racette, B. A. (2011). Reduced uptake of [18F]FDOPA PET in asymptomatic welders with occupational manganese exposure. *Neurology* **76**, 1296–1301.

Racette, B. A., Nielsen, S. S., Criswell, S. R., Sheppard, L., Seixas, N., Warden, M. N., and Checkoway, H. (2017). Dose-dependent progression of Parkinsonism in manganese-exposed welders. *Neurology* **88**, 344–351.

Ramoju, S. P., Mattison, D. R., Milton, B., McGough, D., Shilnikova, N., Clewell, H. J., Yoon, M., Taylor, M. D., Krewski, D., and Andersen, M. E. (2017). The application of PBPK models in estimating human brain tissue manganese concentrations. *NeuroToxicology* **58**, 226–237.

Roels, H. A., Bowler, R., Kim, Y., Claus Henn, B., Mergler, D., Hoet, P., Gocheva, V. V., Bellinger, D. C., Wright, R. O., Harris, M. G., *et al.* (2012). Manganese exposure and cognitive deficits: A growing concern for manganese neurotoxicity. *NeuroToxicology* **33**, 872–880.

Sabati, M., and Maudsley, A. A. (2013). Fast and high-resolution quantitative mapping of tissue water content with full brain coverage for clinically-driven studies. *Magn. Reson. Imag.* **31**, 1752–1759.

Schroeter, J. D., Dorman, D. C., Yoon, M., Nong, A., Taylor, M. D., Andersen, M. E., and Clewell, H. J. (2012). Application of a multi-route physiologically based pharmacokinetic model for manganese to evaluate dose-dependent neurological effects in monkeys. *Toxicol. Sci.* **129**, 432–446.

Silva, A. C., Lee, J. H., Aoki, I., and Koretsky, A. P. (2004). Manganese-enhanced magnetic resonance imaging (MEMRI): Methodological and practical considerations. *NMR Biomed.* **17**, 532–543.

Taylor, M. D., Clewell, H. J., Andersen, M. E., Schroeter, J. D., Yoon, M., Keene, A. M., and Dorman, D. C. (2012). Update on a pharmacokinetic-centric alternative tier II program for MMT-part II: Physiologically based pharmacokinetic modeling and manganese risk assessment. *J. Toxicol.* **2012**, 1.

Teeguarden, J. G., Gearhart, J., Clewell, H. J., Covington, T. R., Nong, A., and Andersen, M. E. (2007). Pharmacokinetic modeling of manganese. III. Physiological approaches accounting for background and tracer kinetics. *J. Toxicol. Environ. Health A* **70**, 1515–1526.

Ward, E. J., Edmondson, D. A., Nour, M. M., Snyder, S., Rosenthal, F. S., and Dydak, U. (2018). Toenail manganese: A sensitive and specific biomarker of exposure to manganese in career welders. *Ann. Work Expo. Health* **62**, 101–111.

Yeh, C.-L., Ward, E. J., Ma, R., Snyder, S., Schmidt-Wilcke, T., and Dydak, U. (2016). P125 whole-brain R1 mapping of manganese in welders—Visualisation of increased Mn levels in the brain. *Occup. Environ. Med.* **73(Suppl. 1)**, A161.